Demonstration of 200 Gbps D-band Wireless Delivery in a 4.6 km 2×2 MIMO system

Yi Wei[1], Jianjun Yu[1*], Mingxu Wang[1], Xianmin Zhao[2], Xiongwei Yang[1], Weiping Li[1], Peng Tian[1], Yang Han[1], Qiutong Zhang[1], Jingwen Tan[1], Bing Zhang[1], Feng Zhao[3], Wen Zhou[1], and Kaihui Wang[1]

[1]*Fudan University, Shanghai 200433, China * jianjun@fudan.edu.cn*

[2]*Harbin Institute of Technology, Harbin, China, 150001*

[3]*School of Automation, Xi'an University of Posts and Telecommunications, Xi'an 710121, China*

Abstract: A 4.6-km 2×2 MIMO wireless system at D-band is experimentally demonstrated with a total data rate of 200 Gbps and a record-breaking capacity-distance product of 920 Gbps·km at D-band.

1. Introduction

In the landscape of next-generation mobile communication networks, Enhanced Mobile Broadband (eMBB) communications stand out as one of the three pivotal application scenarios. This facet is poised to drive an explosive surge in mobile data traffic and transmission rates, all aimed at meeting the ever-growing demands of futuristic technologies such as ubiquitous virtual reality/augmented reality (VR/AR), high-definition 4k/8k video streaming, artificial intelligence, and more. To cater to these burgeoning requirements, the availability of large bandwidths is essential. Millimeter wave (mm-wave) have emerged as suitable contenders due to its considerable available spectrum resources and the potential to achieve long-range and high-speed broadband communications for the future 5G and 6G. Some representative researches on W-band and D-band based on photonics-aided technology have been reported in Ref.[1-11]. Wireless multiple-input multiple-output (MIMO), combined with polarization multiplexing, can effectively double the wireless transmission capacity. The authors in Ref.[12] demonstrated a photonically-enabled independent side-bands D-band 0.2-m wireless transmission and achieved a capacity-distance product of 0.07 Gbps·km. In[13], Li et al. achieved a total bit rate of 184 Gbps in a 0.6-m D-band 2×2 MIMO wireless transmission and the capacity-distance product is 0.11 Gbps·km. In 2019, Li et al. further increased the total capacity to 1.056 Tbps using 4×4 MIMO, and enhanced the capacity-distance product to 3.27 Gbps·km [14].

In this paper, we experimentally demonstrate a high-speed long-haul 2×2 MIMO wireless system at D-band. Using the polarization multiplexing and MIMO techniques, 25-Gbaud 16-QAM signals are successfully transmitted over a 125-GHz 4.6-km wireless link, with a minimum recovered bit error rate (BER) of 2.05×10^{-2}. The maximum data rate is 200 Gbps and the capacity-distance product is enhanced to 920 Gbps·km (200Gbps×4.6km), which is a new record for optical-wireless integration transmission to the best of our knowledge.

2. Experimental setup and DSP

Figure 1(a) demonstrates the experimental setup of the high-speed long-haul 2×2 MIMO wireless system at D-band and digital signal processing (DSP) at the transmitter/receiver side. On the transmitter side, a bit sequence is mapped into the 16-QAM signal. After being up-sampled, root-raised-cosine (RRC) pulse shaped with a roll-off factor of 0.01 and resampled, the digital signal is loaded into a 120-GSa/s AWG to generate the 15-/20-/25-Gbaud 16-QAM signal, which are subsequently boosted by two parallel EAs with 25-dB gain. Two free-running ECLs with a linewidth of 100 kHz, denoted as ECL-1 and ECL-2, are utilized. ECL-1 emits a continuous optical wave at 1550 nm, while the ECL-2 works at 1551 nm. The I/Q modulator, with a 30-GHz 3-dB bandwidth, is driven by a 10 dBm optical carrier emitted from ECL-1 to finish the electro-optic (E/O) conversion. After passing through the PM-EDFA, the optical signal is coupled with the other 14.5-dBm optical carrier emitted from ECL-2 through PM-OC-1. The power of the coupled signal is controlled by the PM-EDFA and an ATT. Subsequently, the coupled signals are divided into two paths using PM-OC-2. In order to effectively eliminates the correlation between the two paths signals, a 2-m PM-ODL is used. After 1-m PM-fiber transmission, the two paths optical signals are input into UTC-PD-1 and UTC-PD-2 [14], respectively, and two 125-GHz mm-wave signals are generated by the photo-mixing technique. Since D-band signals undergo rapid attenuation during free space transmission, it is essential to amplify the 125-GHz mm-wave signals to support the 4.6-km wireless transmission. The amplification of the D-band signals is achieved by a cascaded combination of LNA-1/LNA-2 with a gain of 18 dB and PA-1/PA-2 with the output power of 13 dBm. Afterwards, the two paths mm-wave signals are transmitted into the free space through a pair of

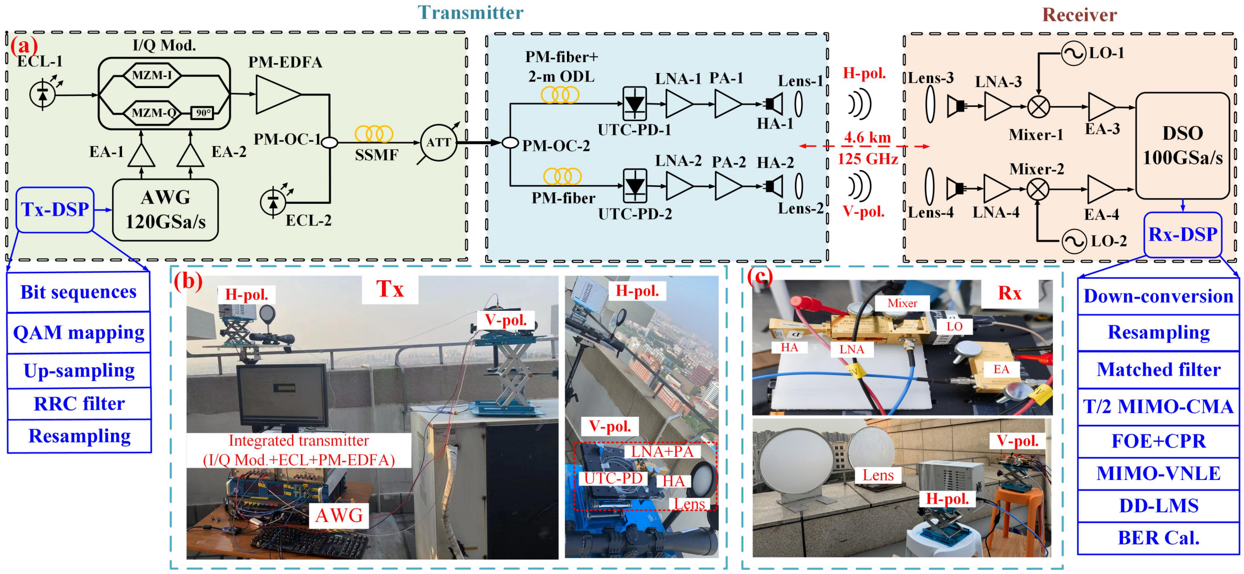

Fig. 1. (a) Experimental setup. AWG: arbitrary waveform generator, ECL: external cavity laser, EA: electrical amplifier, PM-EDFA: polarization-maintaining Erbium-doped fiber amplifier, PM-OC: polarization maintaining optical coupler, ATT: attenuator, ODL: optical delay line, UTC-PD: uni-traveling-carrier photodiode, LNA: low noise amplifier, PA: power amplifier, HA: horn antenna, LO: local oscillator, DSO: digital storage oscilloscope. (b) Transmitter-side DSP. (c)Receiver-side DSP.

horizontally /vertically polarized (H-/V-pol.) HAs with 25-dBi gains. The D-band HA features a relatively small aperture. Therefore, a pair of plano-convex lenses are employed to concentrate the mm-wave beam and maximize the received power of receiver-side HAs. Specifically, Lens-1/Lens-2 has a diameter of 10-cm, while Lens-3/Lens-4 boasts a larger diameter of 60-cm [11]. The experimental scenes at the transmitter side are displayed in Fig. 1(b). It is a sunny day, and the temperature is 24^0C. The transmitters and receivers are located in two different campuses in Fudan University [11].

After 4.6-km wireless transmission, the 125-GHz wireless signals are focused by Lens-3/Lens-4 and then received by the H-/V-pol. HAs, respectively. The H-/V-pol. signals are amplified by LNA-3/LNA-4 with 33-dB gain and down-converted in Mixer-1/Mixer-2. The local oscillator (LO) is 112 GHz and the generated intermediate frequency (IF) is 13 GHz. After down-conversion, the H-/V-pol. IF signals are enhanced by EA-2/EA-3 with 26-dB gain and finally captured by a DSO with 100-GSa/s sampling rate and 33-GHz 3-dB bandwidth. The experimental scenes at the receiver side are demonstrated in Fig. 1(c) [11]. The offline DSP at the receiving side includes down-conversion, resampling, matched filtering, 51-tap T/2 MIMO constant modulus algorithm (MIMO-CMA), frequency offset estimation (FOE), carrier phase recovery (CPR), 183-kernel second-order MIMO Volterra nonlinear equalization (MIMO-VNLE) and 155-tap decision directed least mean square (DD-LMS) equalization.

3. Results and discussion

Figure 2 illustrates the relationship between BER and the input power of PD for H-/V-pol.16QAM signals with baud rates 15-, 20- and 25-Gbaud. For the 15-Gbaud 16-QAM signal, as shown in Fig. 2(a), the BER declines as the input power increases from -3 dBm to -1 dBm, primarily due to the improvement in the signal-to-noise ratio (SNR). However, when the input power continues to increase, the system performance deteriorates rapidly due to the saturation effect of PAs and LNAs. At the power of -1 dBm, the 15-Gbaud H-/V-pol.16-QAM signal achieves a minimum pre-forward-error-correction (pre-FEC) BER of 1.4×10^{-3} and 1.6×10^{-3}, respectively, which is less than 7% hard-decision forward error correction (HD-FEC) threshold of 3.8×10^{-3}, achieving a data rate of 120(=15×4×2) Gbps. The received spectrum of 15-Gbaud H-pol.16-QAM after 125-GHz 4.6-km wireless transmission is embedded in Fig. 2(a) and the recovered constellations of H-/V-pol.16-QAM signals are shown in the inset (i) of Fig. 2(a). As the symbol rate increases, the inter-symbol interference (ISI) phenomenon becomes more obvious and the signal-to-noise ratio gradually decreases, resulting in a decrease in system performance.

As shown in the Fig. 2(b), it is evident that the performance of 20-/25-Gbaud H-/V-pol.16-QAM signals follow a similar trend to that of 15 Gbaud signals. The optimal input power is 0 dBm and at this power point, the minimum pre-FEC BERs of 20-Gbaud H-/V-pol. 16-QAM signals are 7.9×10^{-3} and 8.1×10^{-3}, respectively, while the 25-

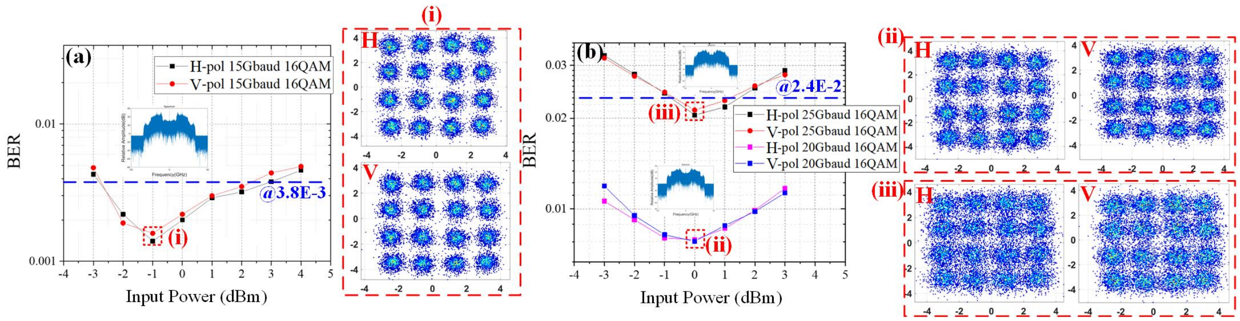

Fig. 2. The relationship between the input power and the BER of (a) 15-Gbaud H-/V-pol.16-QAM signals, (b) 20-/25-Gbaud H-/V-pol.16-QAM signals. Inset: recovered H-/V-pol. constellations of (i)15-Gbaud, (ii)20-Gbaud and (iii)25-Gbaud 16-QAM.

Gbaud H-/V-pol.16-QAM signals achieve the optimal performance of 2.13×10^{-2} and 2.05×10^{-2}, respectively, which meets the 20% soft-decision forward error correction (SD-FEC) threshold of 2.4×10^{-2}. The recovered constellations of 20-/25-Gbaud H-/V-pol.16-QAM signals are shown in the inset (ii) and (iii) of Fig. 2(b). The 2×2 MIMO 25-Gbaud 16-QAM signals reach a maximum bit rate of 200(=25×4×2) Gbps and a single-channel rate of 100(=25 × 4) Gbps. After removing the SD-FEC overheads (20% overhead), the corresponding net bit rate is 174(=25×4×2/1.15) Gbps. It is worth noting that a record-breaking capacity-distance product of 920(=200×4.6) Gbps·km is realized at D-band.

4. Conclusions

We experimentally demonstrated a photonics-assisted 2×2 MIMO wireless system at D-band, where a maximum bit rate of 200 Gbps is achieved. The transmission distance is 4.6 km and the achieved capacity-distance product is 920 Gbps·km. To the best of our knowledge, this is the first time to reach 920 Gbps·km capacity-distance product at D-band.

This work was supported by the National Natural Science Foundation of China (No. 62305067, No. 61935005, and No. 61835002, No. 62375219, No. 62331004).

References

[1] X. Li et al., in Proc. *OFC PDP*, Th5A.5 (2015).
[2] X. Li et al., in Proc. *ECOC*, pp.1-3 (2015).
[3] X. Li et al., *J. Lightw. Technol.,* 36, 50-56 (2018).
[4] W. Li et al., *J. Lightw. Technol.,* 41, 4010-4016 (2023).
[5] M. Wang et al., *Opt. Lett.* 48, 3997-4000 (2023).
[6] W. Li et al., in Proc. *ECOC*, We1F.6 (2022).
[7] L. Juan et al., *IRMMW-THz*, pp.1-2 (2021), *DOI:*10.1109/IRMMW-THz50926.2021.9567641.
[8] Zhanget al., *Sensors* 22(23), pp. 9514 (2022).
[9] M. Wang et al., *J. Lightw. Technol., DOI: 10.1109/JLT.2023.3325336.*
[10] Y. Wei et al.*OECC PDP*, pp.1-4 (2023).
[11] W. Li et al., *IEEE Trans. Microw. Theory Techn., doi: 10.1109/TMTT.2023.3267547.*
[12] R. Puerta et al., in Proc. OFC, Tu3B.3 (2017).
[13] X. Li et al., *IEEE Photon. J.,* 8, pp. 1-10 (2016).
[14] X. Li *et al.*, *J. Lightw. Technol.,* 37, pp. 196-204 (2019).